Developmental Biology **210,** 322–338 (1999)
Article ID dbio.1999.9287, available online at http://www.idealibrary.com on IDEAL®

Neural Crest Development in Zebrafish

Chris J. Cretekos and David Jonah Grunwald
Department of Human Genetics, University of Utah School of Medicine, Salt Lake City, Utah 84112

***alyron*^{z12} (*aln*) is a recessive lethal mutation that affects early stages of neural crest development in the zebrafish. *alyron* appears to be an insertional mutation as the mutation was generated following microinjection of plasmid DNA into one-cell embryos and the stably integrated transgenic sequences are closely linked to the mutation. The insertion site harbors multiple copies of the plasmid sequence that have experienced complex rearrangements. Host–insert junction fragments have been molecularly cloned and host sequences adjacent to the transgene have been used to map the mutation to the distal arm of linkage group 15. *alyron* function is required cell-autonomously in the neural crest lineage. *alyron* mutants have a severe but not complete deficit of premigratory neural crest as judged by reduced expression of several markers associated with early stages of neural crest development. Lack of premigratory neural crest is likely to account for the two most conspicuous characteristics of *alyron* mutants: the absence of body pigmentation and the inability to affect blood circulation. The neural crest phenotype of *alyron* mutants resembles that observed in mouse mutants that lack *Pax-3* or both *Wnt-1* and *Wnt-3a* function, and expression of the zebrafish homologues of these genes is greatly reduced in the dorsal neural keels of *alyron* mutants. In contrast, ventral neural keel identity appears unaffected. Given our findings that the mutation is unlinked to *pax* or *wnt* genes that have been described in the zebrafish, we propose that *alyron* is a novel gene function required for the specification and/or proliferative expansion of neural crest progenitors.**

Key Words: **zebrafish mutant; insertional mutagenesis; neural crest; pigmentation; heart.**

INTRODUCTION

The neural crest is a multipotential progenitor cell population that forms at the lateral edges of the vertebrate neural plate and gives rise to a wide array of neural and nonneural tissues (LeDouarin, 1982). Upon neural tube closure, neural crest cells migrate along stereotypical pathways to sites where they undergo terminal differentiation. Cranial neural crest contributes to the formation of pigmented tissue, branchial arches and craniofacial cartilage, cranial ganglia, the enteric nervous system, and portions of the heart and the ear. Trunk neural crest cells contribute to pigmented tissue, endocrine tissue, and the peripheral nervous system including the dorsal root ganglia. Defects in the origin, proliferation, migration, or differentiation of neural crest cells contribute to a wide spectrum of developmental syndromes in humans and other animals (Creazzo *et al.*, 1998; Hong, 1998; Anderson, 1997; Read and Newton, 1997; Schilling, 1997).

Analyses of mutants defective in neural crest development and experimental manipulations of tissues and growth factors that contribute to patterning of the neuraxis have indicated an intimate association between the establishment of dorsal neural tube identity and the generation of the neural crest. BMP and perhaps Wnt and FGF signals appear to promote induction of both neural crest and dorsal neural tube (Liem *et al.*, 1995, 1997; Mayor *et al.*, 1995, 1997; Mehler *et al.*, 1997; Chang and Hemmati-Brivanlou, 1998; LaBonne and Bronner-Fraser, 1998). Consistent with this hypothesis, analysis of zebrafish mutants and *Xenopus* embryos with altered levels of BMP signaling indicates that specific levels of BMP are likely required to induce neural crest (Morgan and Sargent, 1997; LaBonne and Bronner-Fraser, 1998; Nguyen *et al.*, 1998). In response to the inductive signals, a set of genes believed to confer dorsal neural tube identity, such as *Wnt-1*, *Wnt-3a*, *Pax-3*, and *Pax-7*, become expressed widely in the dorsal neural tube, including the region where neural crest progenitors reside. The dorsal identity genes play an essential role in neural crest development. Expansion or diminution of the *Wnt* expression domain, accomplished by ectopic expression or mutation, leads to a corresponding increase or decrease in

0012-1606/99 $30.00

premigratory neural crest cells or their differentiated derivatives (Augustine *et al.*, 1993; Ikeya *et al.*, 1997; Saint-Jeannet *et al.*, 1997; LaBonne and Bronner-Fraser, 1998). Similarly, loss of *Pax-3* or *Pax-7* gene function results in a substantial deficit of neural crest cells (Franz and Kothary, 1993; Tremblay *et al.*, 1995; Mansouri *et al.*, 1996; Serbedzija and McMahon, 1997). Because loss of function of the dorsal identity genes results in dramatically reduced numbers of neural crest, it is believed that these genes function in the execution/maintenance of the neural crest fate and/or in the proliferative expansion of the neural crest progenitors.

Whereas the loss-of-function *Pax* and *Wnt* mutants indicate that these genes are essential for neural crest development, their exact roles are obscure since the mutations do not completely eliminate the neural crest. The incomplete effects of these mutations might result from heterogeneity within the precursor population, the expression of gene family members with overlapping or redundant functions, or the existence of independent pathways that together promote full levels of neural crest specification. The possibility that the *Pax* and *Wnt* genes regulate each others' expression, indicated by the finding that *Pax-3* gene expression is downregulated in *Wnt-1/Wnt-3a* double mutants (Ikeya *et al.*, 1997), further confounds interpretation of each gene's unique role.

Expression of the dorsal identity genes does not directly establish the neural crest lineage, as only a subset of the cells expressing these genes give rise to neural crest. As indicated by the *mindbomb/whitetail* mutant of zebrafish, which displays supernumerary dorsal primary sensory neurons along with a marked reduction in premigratory neural crest (Jiang *et al.*, 1996; Schier *et al.*, 1996), a process of lateral inhibition, perhaps involving Notch/Delta signaling (reviewed in Lewis, 1996), appears to be required for the subdivision of the dorsal neural tube into different cell types.

To better understand the factors that contribute to establishment of the neural crest, we need more mutants that affect early stages in neural crest specification. Here we describe a new zebrafish mutant with a severe deficit of early neural crest. The mutation, called *alyron* [from the Greek, meaning without (a rooster's) crest], is the first embryonic lethal mutation induced by DNA microinjection to be described in zebrafish. *alyron* is phenotypically distinguishable from the large number of neural crest mutants that has been identified already in zebrafish (Neuhauss *et al.*, 1996; Piotrowski *et al.*, 1996; Schilling *et al.*, 1996a,b; Kelsh *et al.*, 1996; Odenthal *et al.*, 1996; Henion *et al.*, 1996; Chandrasekhar *et al.*, 1997). Moreover, since *alyron* is distinct from the *Wnt* and *Pax* genes known to be involved in dorsal neural tube identity in the mouse, it appears to be a newly identified regulator of early neural crest development. As with other genes shown to be essential for neural crest development, *alyron* is required for normal expression levels of dorsal neural tube identity genes.

MATERIALS AND METHODS

Fish Maintenance

Zebrafish stocks were raised and maintained as described in "The Zebrafish Book" (Westerfield, 1994). The transgenic line described here was generated in the Ekkwill wild-type strain described previously (Riley and Grunwald, 1995) and was propagated by mating with Ekkwill wild-type individuals except where noted. The pigmentless *albino*^{b4} strain was obtained from C. Kimmel. Embryos were cultured at 28.5°C and developmental stages are given as hours postfertilization (h) at this temperature.

A Screen for Insertional Mutants

The *alyron*^{z12} mutation was recovered in a screen for insertional mutations in zebrafish. Potentially transgenic founders were generated by microinjection of linearized plasmid DNA into the cytoplasm of one-cell embryos. The injection solution contained 100 mM KCl, 3% green food color (used to estimate injection volume), and 100 μg/ml pSLAC, linearized by restriction at the unique *Eco*RI site (Fig. 7A). About 0.4 nl was injected per embryo. pSLAC consists of a gene fusion of the intron 1 branch point and splice acceptor from the human β-globin gene (Reed and Maniatis, 1986), the *Escherichia coli* Lac Z coding sequence, and a polyadenylation signal from SV40, inserted into the pSP72 vector (Promega). Injected embryos were raised to adulthood and mated with WT partners, and the genomes of their progeny were screened for the presence of plasmid sequences by PCR. Twelve of 73 G0 founders transmitted plasmid-derived sequences to a fraction of their progeny. The fraction of progeny that inherited plasmid DNA ranged from 2 to 13%, with a mean of 5%, indicating that the germ lines of the founders were mosaic (Stuart *et al.*, 1990; Culp *et al.*, 1991; Bayer and Campos-Ortega, 1992).

True breeding transgenic lines were established from each of the 12 germline-transgenic founders. F1 offspring that inherited the plasmid sequences were identified by screening genomic DNA prepared from fin biopsies. F1 offspring appeared to be true heterozygotes, transmitting transgenic sequences to 50% of their offspring. For example, all plasmid sequences present in one transgenic line, SLAC113, have segregated as a single locus in a stable Mendelian pattern for more than nine generations.

Carriers from within each line were intercrossed to uncover recessive phenotypes. Intercross progeny from the SLAC113 transgenic line displayed a novel lethal syndrome. One-fourth of the progeny produced from matings between heterozygous carriers of the SLAC113 transgene exhibited the lethal syndrome (2010 mutants/8082 intercross progeny screened = 24.9%). We therefore conclude that the SLAC113 line harbors a recessive lethal mutation, which we have termed *alyron* (*aln*).

Detection of Transgenic Plasmid Sequences by PCR or Dot-Blot

DNA was extracted from individual 24-h embryos, pools of ten 24-h embryos, or individual fin biopsies by digestion for 2 h at 55°C in 50 μl of 1× PCR buffer (50 mM KCl, 1.5 mM $MgCl_2$, 20 mM Tris–HCl, pH 8.3) supplemented with 0.1% Nonidet P40, 0.1% Tween 20, and 0.1 mg/ml proteinase K. DNA preparations were boiled 10 min to inactivate the proteinase K and centrifuged at 14,000*g* to pellet debris, and the supernatant was stored at 4°C until use. For PCR analysis, 100–200 ng of each DNA preparation

was used per reaction and two reactions were performed per DNA preparation. To detect plasmid-derived sequences, pSLAC specific primers SLAC-A (5′-GCACTGACTCTCTTCCTTTG) and SLAC-B (5′-GCTGCAAGGCGATTAAGTTG) were used (positions indicated as A and B in Fig. 7A). As a control for DNA template quality, each preparation was also amplified with a primer pair directed against zebrafish *retinoic acid receptor-2* (gift from S. Stachel). For dot-blot analysis of fin biopsy DNA, the entire DNA preparation was used on blots prepared and hybridized as described by Stuart *et al.* (1988).

Genetic Mosaic Analysis

Genetic mosaics were constructed by aspirating 25–50 cells from labeled embryos (donors) at the 2- to 4000-cell stage and transplanting into unlabeled siblings or equivalently staged *albino* embryos (hosts). All manipulations and incubations were carried out in egg water (Westerfield, 1994) supplemented with 10 mM Hepes, pH 7.2, 100 U/ml penicillin G, and 0.1 mg/ml streptomycin sulfate (Gibco). To label donors, intercross progeny of *alyron*/+ animals were microinjected with about 0.4 nl of 25 mg/ml FITC–dextran (2 MD MW; Sigma) in 100 mM KCl at the 1-cell stage. Donors and hosts were immobilized in 2% methylcellulose in depression slides for cell transplantation and then isolated into individual wells of 24-well plates for later genotyping. The transplanted cells were placed either close to the margin of the blastoderm to increase their probability of developing as blood (Lee *et al.*, 1994) or about halfway between the animal pole and the margin to increase their probability of developing as neural crest (Woo and Fraser, 1995). Donors and hosts were genotyped at 24 h by inspection of phenotype. Mosaic embryos were screened under epifluorescence microscopy and the contribution of the donor cells to identifiable tissues was noted. In some cases mosaic embryos were fixed in 4% paraformaldehyde and the fluorescent lineage tracer was converted to HRP reaction product immunohistochemically according to the method of Garton and Schoenwolf (1996).

In Situ Hybridization, Immunohistochemistry, and Photomicrography

RNA *in situ* hybridization was carried out as described by Hug *et al.* (1997). The following gene probes were used: *AP-2* (Furthauer *et al.*, 1997), *c-ret* (Bisgrove *et al.*, 1997; Marcos-Gutierrez *et al.*, 1997), *dlx-2* (Akimenko *et al.*, 1994), *fkd-6* (Odenthal and Nusslein-Volhard, 1998), *flk-1* (Liao *et al.*, 1997), *goosecoid* (Stachel *et al.*, 1993), *isl-1* (Inoue *et al.*, 1994; Appel *et al.*, 1995), *isl-2* (Appel *et al.*, 1995), *krox-20* (Oxtoby and Jowett, 1993), *pax-3* and *pax-7* (Seo *et al.*, 1998), *snail-2* (Thisse *et al.*, 1995), *sonic hedgehog* (Krauss *et al.*, 1993), *trp-2* (R. Kelsh, unpublished), *wnt-1* (Molven *et al.*, 1991; Dorsky *et al.*, 1998), *wnt-3a* (R. Dorsky and R. Moon, unpublished), and *zash-1a* and *zash-1b* (Allende and Weinberg, 1994). Immunohistochemistry was carried out essentially as described by Trevarrow *et al.* (1990). Mouse anti-fluorescein and secondary antibodies were obtained from Jackson ImmunoResearch. Xanthophore autofluorescence was visualized according to the method of Epperlein *et al.* (1988). Photomicrographs were captured as color slides using a Zeiss Axioplan microscope equipped with DIC and epifluorescence optics. Slides were digitally scanned, and images were processed with the aid of Adobe Photoshop 3.0 software.

Cell Lineage Analysis and Confocal Microscopy

DiI labeling of hindbrain neural crest was accomplished by application of 125 μg/ml DiI (Molecular Probes) in 5% DMSO, 95% ethanol (D. Darnell and G. Schoenwolf, personal communication) onto the neural folds at axial positions between the isthmus and the first somite furrow at the one- to two-somite stage of development. Bodipy counterstaining was carried out as described by Cooper and D'Amico (1996), using 1 mg/ml Bodipy 505/515 (Molecular Probes) in DMSO as a 100× stock solution. Confocal z-series were collected using a Bio-Rad MRC1024 confocal apparatus on a Zeiss Axioplan microscope. Images were subsequently processed using Adobe Photoshop 3.0 software.

Fluid Circulation Analysis

Cardiovascular fluid circulation was examined by microinjection of about 1 nl of 25 mg/ml FITC–dextran (Sigma) in 100 mM KCl into the common cardinal vein (injection site indicated in Figs. 5C and 5D). Twenty 26-h mutant embryos and 20 wild-type siblings were dechorionated and immobilized in 3% methylcellulose for microinjection. Each dye-injected embryo was inspected under epifluorescence immediately following microinjection and the progress of dye through the circulatory system noted. To document the results, some examples were anesthetized in 0.2 mg/ml tricane (Westerfield, 1994), remounted, and photographed under epifluorescence.

Southern Analysis

Southern analysis was conducted using several gel and blotting conditions, depending on the size range of DNA fragments to be separated. Field inversion gel electrophoresis (FIGE) was used to separate DNA fragments of high molecular weight, using a Hoefer Model PC750 pulse controller, 2.1-s forward and 0.7-s backward field pulses of 18 V/cm at 4°C for 16–18 h. High-molecular-weight DNA was prepared by digestion of dissected adult soft tissues in agarose plugs essentially as described for mouse soft tissues in Ausubel *et al.* (1989). DNA for standard Southern analysis was prepared as described in Westerfield (1994). Southern blots of FIGE gels and standard gels were generated as described in Monaco (1995) and Sambrook *et al.* (1989). All gels were transferred onto Duralon membrane (Stratagene).

Junction Fragment Cloning

The *Spe*I-end junction fragment was cloned using a modification of the linker/adapter PCR method described in Vooijs *et al.* (1993) (see Fig. 7D). Genomic DNA from *aln*/+ animals was digested with *Spe*I, which fails to cleave pSLAC. An *Spe*I-end compatible linker was generated by digestion of pBluescript SK− (Stratagene) with *Spe*I and *Pvu*II followed by agarose gel purification of a 247-bp fragment containing the T3 promoter and a portion of the multiple cloning site. The linker was ligated to the ends of *Spe*I-digested genomic DNA in a 1000:1 molar ratio using T4 DNA ligase, assuming an average *Spe*I-digested genomic fragment of about 8 kbp. The DNA was then digested with *Bsr*DI to liberate the junction fragment, and sequences spanning the junction were amplified in two rounds of PCR using the T3 primer (Stratagene) as the linker-specific primer and two reverse primers specific for plasmid sequences predicted to be near the junction, SLAC-B (5′-GCTGCAAGGCGATTAAGTTG) and SLAC-C (5′-

GCTCTAGACGTTGTAAAACGACGGG). The resulting 2.1-kbp amplification product was agarose gel purified and cloned into pBluescriptII KS− (Stratagene).

Linkage Analysis and Genetic Mapping

Oligomer PCR primers (J191: F = 5′-CAGGTGTACCTAATAAAGTGGC, R = 5′-TATTTCTCTGTTAATGTCATCCC) specific for host sequences immediately adjacent to the SLAC113 transgene were used to identify the segregation of *aln* in a radiation hybrid (RH) panel (Kwok *et al.*, 1998; Research Genetics). Analysis of the segregation data was kindly performed by R. Geisler and P. Haffter (http://wwweb.mpib-tuebingen.mpg.de/abt.3/haffter_lab/rh_mapping.html). To determine whether candidate genes were linked to *aln*, the segregation of *wnt-1, wnt-3a, pax-3*, and *pax-7* sequences within the RH panel was determined. The following oligomer primers were used: *wnt-1*, F = 5′-GGGTATAGTGAATGTGGCATC, R = 5′-CTCGGTTGACAATTTTGCCAA; *wnt-3a*, F = 5′-TGATCGGCGACTACATGAAGG, R = 5′-TGGCACTTTTCTTTGCGCTTC; *pax-3*, F = 5′-GTGCATCAGTCTGGGCTTG, R = 5′-GCTGATGGAGGGGTTCACT; *pax-7*, F = 5′-ACACTACACCGCTAAAAACG, R = 5′-GCCCCCTAAAATAAAAATCC.

RESULTS

Overview of alyron Mutant Phenotype

alyron^{z12} (*aln*) is a recessive lethal mutation that was recovered in a screen for insertional mutations induced following DNA microinjection into zebrafish embryos (see Materials and Methods for details). The most conspicuous morphological defects of mutant embryos are lack of body pigmentation, reduced eye pigmentation, failure of blood cells to enter circulation, and pericardial edema (Figs. 1A–1D). Several lines of evidence indicate that lack of body pigmentation results from the absence of chromatophores, the neural crest-derived pigment cells, rather than a general defect in pigmentation. Although the pigmented retinae of mutant eyes accumulate black pigment, albeit at reduced levels, >90% of the mutant embryos never develop melanophore pigmentation (Fig. 1D). In mutant embryos that produce a few melanophores (average of 14 melanophores found on 10/112 mutants scored), the melanophores are of normal morphology and are pigmented (data not shown). Thus, the mutation appears to block the production rather than the differentiation of these cells. Consistent with this interpretation, cells in the pigmented retinae but not on the bodies of mutant embryos express *tyrosinase related protein-2* (*trp-2*), a gene involved in melanin biosynthesis (Figs. 1E and 1F). Finally, multiple chromatophore lineages are missing in mutants. In addition to the absence of the melanophores, mutants lack xanthophores, which normally can be detected at 2 days of development by virtue of the autofluorescence of their pteridine (yellow) pigment (Figs. 1G and 1H). Iridophore development could not be scored, as these cells are first distinguishable at about 3 days, the time that mutant embryos die.

Mutant embryos also display a cardiovascular defect. Blood precursors differentiate, but do not enter circulation; instead they accumulate above the yolk sac (arrowheads in Figs. 1C and 1D). As with a number of other zebrafish mutants with circulatory defects, pericardial edema develops. Several more subtle defects are also consistently exhibited by *aln* homozygotes. The otic vesicles of mutant embryos are smaller and rounder than normal and often lack or display tiny otoliths (Figs. 1A–1D). Beginning at about 22 h, mutant embryos develop at a detectably slower rate than their unaffected siblings, as judged by the formation of somites (Cretekos, 1998). During the second day of development the central nervous system becomes necrotic. On the third day of development the heart beat becomes slower and more erratic than normal. By 3–3.5 days, all mutant embryos have died, as judged by cessation of heart beat and developmental arrest.

Genetic Mosaic Analysis of alyron Function

The absence of pigment cells and absence of circulating blood cells exhibited by *aln* mutants are also characteristics found together in mouse mutants in which either c-Kit receptor signaling or *Pax-3* gene function has been compromised (Auerbach, 1954; Epstein *et al.*, 1991; Besmer *et al.*, 1993; Fleischman, 1993; Conway *et al.*, 1997). In each of the relevant mouse mutants, a distinct set of primary cell defects are responsible for the combined phenotype. To determine the cellular basis of the morphological defects seen in *aln* mutant embryos we carried out genetic mosaic analysis. Genetic mosaics were made by transplantation of 25–50 fluorescently labeled WT or mutant cells into unlabeled hosts at the late blastula stage of development, a time at which fate-mapping studies had shown most cells to be pluripotent (Kimmel and Warga, 1987; Ho and Kimmel, 1993).

To determine whether *aln* mutant embryos could support chromatophore development, we assessed the ability of WT blastomeres to develop as melanophores and xanthophores in WT or *aln* mutant hosts. *albino* embryos were used as WT hosts because the lack of black melanin in these otherwise normal embryos made it easy to score the development of donor-derived WT melanophores. No significant difference was seen between the frequency of WT cells differentiating as melanophores in either *albino* or *aln* hosts. In 25 of 107 (23%) mosaics generated from transplantation of WT cells into *albino* hosts (WT → *albino*) and in 23 of 85 (27%) WT → *aln* mosaics WT donor cells differentiated as melanophores. Figure 2A shows an example of a WT → *aln* mosaic in which labeled WT cells have differentiated as pigmented cells whose morphology and position are characteristic of melanophores. All melanophores produced in WT → *aln* mosaics appeared to be of WT origin as judged by simultaneous expression of black melanin and brown HRP product produced following immunohistochemical detection of the lineage tracer marking the donor cells (Figs. 2B and 2C). Eight of the WT → *aln* mosaics with donor-derived melanophores were further analyzed for the

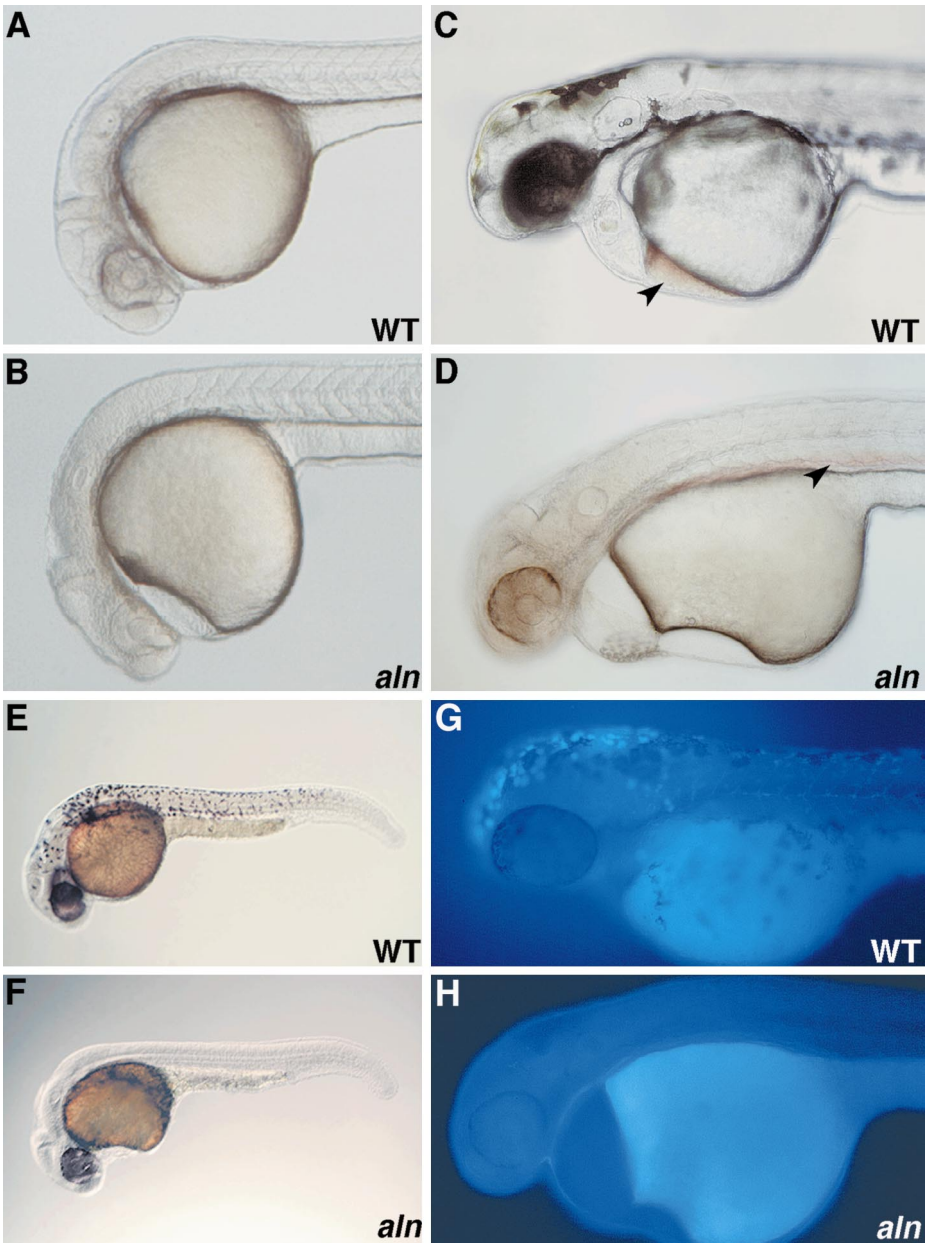

FIG. 1. Overview of *aln* mutant phenotype. (A, B) WT sibling (A) and *aln* mutant (B) 24-h embryos. *aln* mutants display delayed pigmentation in the eye, a smaller than normal otic vesicle, and an enlarged pericardial cavity. In addition, mutant embryos are slightly delayed developmentally, having on average two less somites than their WT siblings at 24 h (not shown). (C, D) WT sibling (C) and *aln* mutant (D) 48-h embryos. *aln* mutants lack body pigmentation, do not circulate blood, and usually have reduced eye pigmentation. Differentiated blood cells accumulate above the yolk cell in mutants (arrowhead in D), whereas they are visible flowing into the inflow tract of the heart in WT embryos (arrowhead in C). (E, F) Expression of *trp-2* in WT sibling (E) and *aln* mutant (F) 26-h embryos detected by RNA *in situ* hybridization. At 26 h, *trp-2* expression is detectable in the retina but not elsewhere in *aln* mutants. (G, H) Xanthophores, identified by their bright blue autofluorescence under DAPI epifluorescence, are seen on the dorsal surface of the head of WT 48-h embryos (G), but are not detected in *aln* mutants (H).

formation of xanthophores. In each of the eight mosaic embryos, WT-derived xanthophores were observed (data not shown). Thus, *aln* mutant and WT embryos are similar in their ability to support the development of melanophores and xanthophores.

Although WT progenitors could develop as chromato-

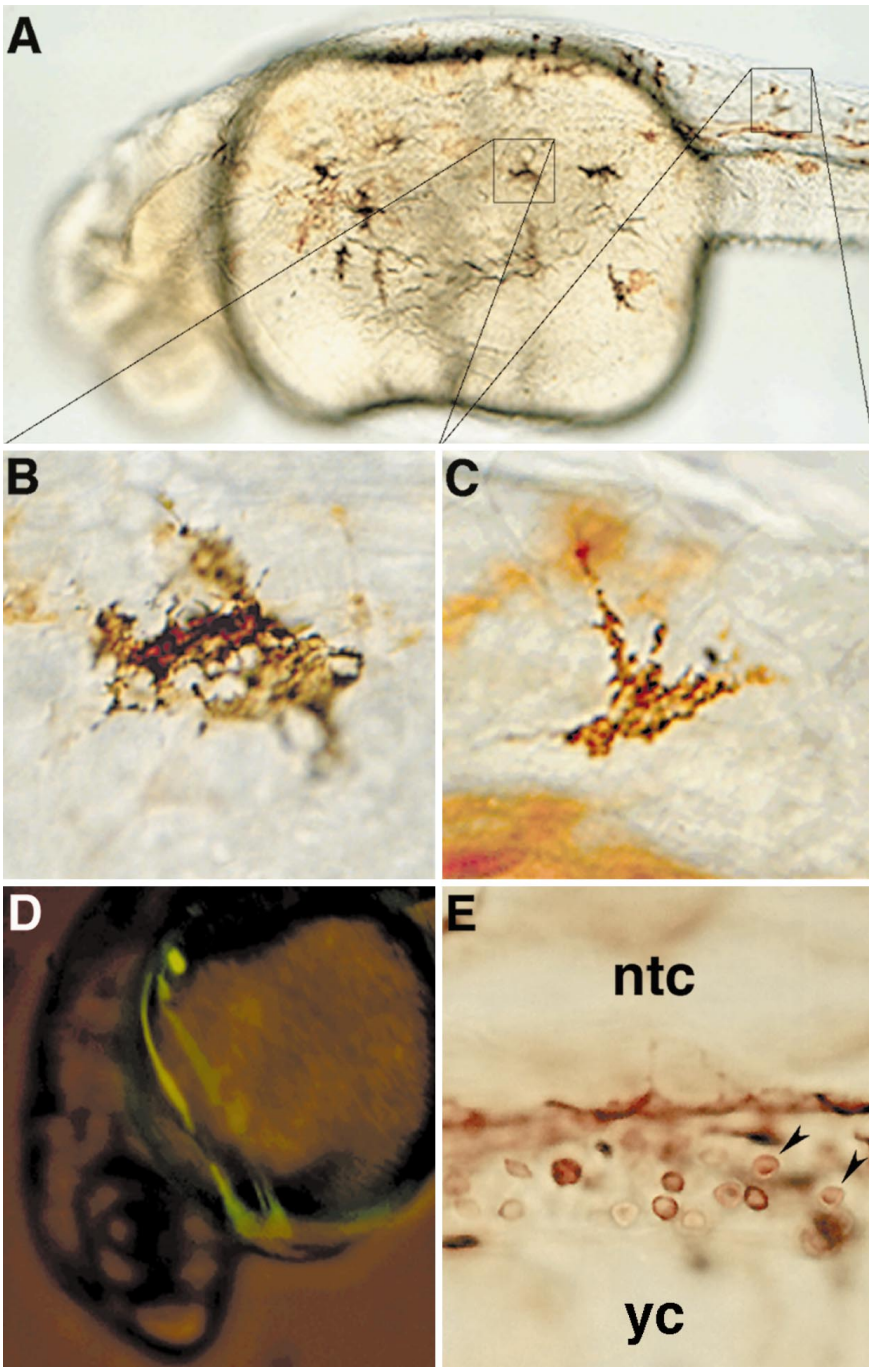

FIG. 2. Genetic mosaic analysis. (A) Dorsolateral view of a WT → *aln* 26-h mosaic that displayed melanophores. The FITC–dextran lineage tracer, indicating WT donor cells, has been detected immunohistochemically (brown). (B, C) Higher magnification views of two of the melanophores pictured in A, showing that WT donor cells (brown) produce melanophores displaying normal morphology and pigmentation (black) in *aln* hosts. (D) Backlit FITC epifluorescence view of a living *aln* → WT 26-h mosaic. The mutant donor cells that differentiated as blood circulate normally, indicated by the green streaks generated by the passage of labeled cells through the circulatory system during a long exposure. (E) High-magnification view of the intermediate cell mass region of a WT → *aln* mosaic (anterior to the left, dorsal to the top). The FITC–dextran lineage tracer has been detected immunohistochemically. WT cells (brown) that display typical erythroid morphology (arrowheads) fail to circulate and instead accumulate between the yolk cell (yc) and the notochord (ntc).

phores in mutant hosts, *aln* progenitors never produced chromatophores in WT hosts. *aln*-derived melanophores were not detected in 44 *aln* → *albino* mosaics, indicating that *aln* function is required cell-autonomously in the chromatophore lineage. Given the lack of melanophores and xanthophores in *aln* mutants, and the finding that small numbers of WT donor cells give rise to both chromatophore types, it is likely that *aln* is required in a precursor cell that contributes to multiple types of differentiated pigment cells.

In contrast to the cell-autonomous requirement for *aln* function in pigment cell precursors, *aln* is not required in blood cell precursors. When *aln* mutant cells differentiated as blood in WT hosts ($n = 6$), the mutant cells entered circulation normally (Fig. 2D). When WT donor cells differentiated as blood in *aln* mutant hosts ($n = 5$), the WT cells failed to circulate and were found intermixed with host blood cells in the space between the yolk cell and the embryo proper (Fig. 2E). In sum, mosaic analyses indicate that aln^+ function is required in the pigment cell lineage but not the blood cell lineage.

Analysis of Circulatory Defect

The impaired circulation exhibited by alyron mutants could result from a primary defect in neural crest development, as neural crest derivatives are important for normal heart function (Conway *et al.*, 1997; reviewed in Creazzo *et al.*, 1998). We examined the possibility that *alyron* mutant embryos are defective in heart function. Although mutant hearts contract with normal rhythm through the second day of development and the major blood vessels appear to be formed normally as judged by the expression of the vascular endothelium marker *flk-1* (Figs. 3A and 3B), little or no fluid circulation through the hearts of *aln* mutant embryos takes place. Fluid circulation was analyzed by following the progress of fluorescein–dextran dye injected into the common cardinal vein of 26- to 28-h embryos. In wild-type embryos, dye passes through the heart and has circulated through the head, trunk, and tail vasculature within about 30 s (Figs. 3C and 3C′). In mutant embryos, the dye was readily drawn into the heart, but little, if any, circulated beyond the heart, even after 30 min of analysis (Figs. 3D and 3D′). Thus, it appears that the lack of blood circulation in *aln* mutants is the result of a defect in heart function.

alyron Homozygotes Are Deficient in Premigratory Neural Crest

As a defect in neural crest development could account for both the absence of chromatophores and the ineffective heart function observed in *aln* mutants, we analyzed expression of three early markers of neural crest: *snail-2* (the zebrafish homologue of *slug;* Nieto *et al.*, 1994; Thisse *et al.*, 1995), *AP-2* (Furthauer *et al.*, 1997), and *fkd-6* (Odenthal and Nusslein-Volhard, 1998). *snail-2/slug* is expressed in premigratory and early migrating neural crest in all vertebrates that have been examined, and its function is required for the normal migration and development of neural crest in the chick embryo (Nieto *et al.*, 1994; Sechrist *et al.*, 1995). In addition, the gene is expressed in head and paraxial mesoderm. *fkd-6* is expressed in a pattern that is nearly identical to that of *snail-2*. *AP-2* is expressed in presumptive neural crest from the neurula stage onward.

Since the neural crest arises in a rostral-to-caudal wave of development, embryos generated by intercrosses of *aln/+* heterozygotes were analyzed by whole-mount *in situ* hybridization at several developmental time points. Prior to the time at which mutant and WT embryos could be distinguished, one-fourth of the intercross progeny displayed a marked reduction in the expression of *snail-2* along the dorsal midline of the head and anterior trunk (Figs. 4A, 4B, 4I, and 4J). By 18 h, mutant and WT embryos could be distinguished unambiguously because mutants have reduced expression of *trp-2* in the retina. Analysis of 18-h intercross progeny doubly stained for *trp-2* and *snail-2* indicated that mutant embryos have severely reduced *snail-2* expression along the dorsal midline of the trunk and tail (Figs. 4C and 4D). Expression of *snail-2* in the developing somites appeared unaffected in mutants. Analysis of 18-h intercross progeny doubly stained for *trp-2* and *AP-2* (Figs. 4E and 4F) or *trp-2* and *fkd-6* (Figs. 4G and 4H) showed similarly reduced expression along the dorsal midline of the trunk and tail.

Analysis of *snail-2* expression in neural keels of 12-h (Figs. 4I and 4J) and 20-h (Figs. 4K and 4L) embryos and in transverse sections taken through the nascent somite of sibling WT and mutant embryos (Figs. 4M and 4N) indicated that the dorsal neural keels of mutant embryos have a dramatically reduced number of *snail-2*-expressing cells, which express reduced levels of *snail-2* mRNA. In addition, analysis of sectioned material confirmed that *snail-2* expression is reduced specifically in the dorsal neural keel and appears to be expressed normally in the developing somites.

Neural Patterning in alyron Mutant Embryos

The severe reduction in *snail-2* expression above the neural keel of mutant embryos indicated an early defect in the specification of the neural crest, such as might arise from incorrect patterning of the neuraxis. Rostrocaudal patterning of the nervous system appeared normal in mutants, as judged by expression of *zash-1a*, *zash-1b*, and *dlx-2* in the fore-, mid-, and hindbrain (Figs. 5A and 5B and data not shown) and *krox-20* in rhombomeres 3 and 5 of the hindbrain (Figs. 5C and 5D). General characteristics of dorsoventral patterning in the nervous system also appeared normal in mutants. Ventral-specific cell types, including *sonic hedgehog*-expressing cells in the ventral brain and floorplate (Figs. 5E and 5F) and *c-ret*-expressing primary motoneurons in the ventral neural keel (Figs. 5G and 5H), appeared normal in mutants. Transverse sections of the trunk revealed that the relative positions within the neural keel of the *isl-2*-expressing ventral primary motoneurons

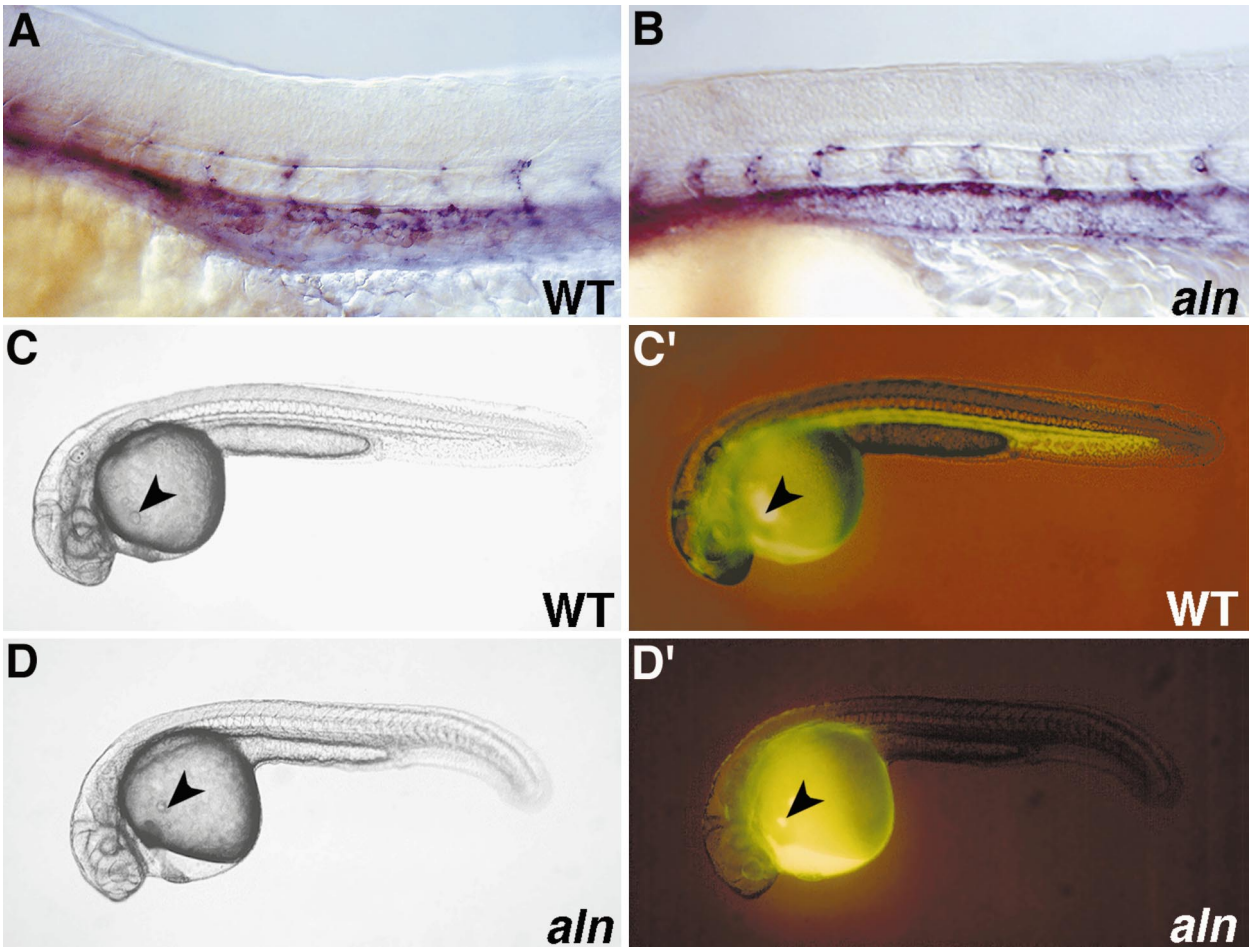

FIG. 3. Analysis of cardiovascular defect. (A, B) WT sibling (A) and *aln* mutant (B) 24-h embryos stained for *flk-1* expression by RNA *in situ* hybridization. The major blood vessels appear to be formed normally in mutant embryos. (C–D′) Fluid circulation was visualized by microinjection of fluorescent dye into the common cardinal vein. The site of dye injection in a 26-h WT sibling (C, C′) and *aln* mutant (D, D′) is indicated by arrowheads. (C′) Epifluorescence view of the WT embryo pictured in C, photographed about 1 min after injection. Dye has passed through the heart, circulated through the head, and traveled to and returned from the tail. (D′) Epifluorescence view of the *aln* mutant embryo pictured in D, photographed 30 min after injection. Dye was drawn into the heart, but little if any circulated further.

and dorsal Rohon-Beard sensory neurons were unaffected in mutant embryos (Figs. 5I and 5J).

Despite apparent normal patterning of the nervous system, expression of several genes associated with dorsal neural tube identity was reduced in *aln* mutants. Expression levels of *pax-3* and to a lesser extent *pax-7* genes that mark the dorsal neural keel (Seo *et al.*, 1998) are reduced in mutant embryos (Figs. 6A and 6B; data not shown). Similarly, *wnt-1* expression in the dorsal neural keel is also reduced at early stages of development in mutant embryos (Figs. 6C and 6D), and *wnt-3A* expression in the dorsal neural keel becomes strongly reduced at later stages (Figs. 6E and 6F).

We examined whether the reduced expression of the four regulatory genes that mark the dorsal neural keel correlated with the loss of identifiable dorsal neural cell types in addition to premigratory neural crest. Rohon-Beard (RB) sensory neurons are among the earliest cells to differentiate in the neural keel, arising adjacent to the neural crest (Grunwald *et al.*, 1988). These cells can be distinguished unambiguously as the only cells in the 24-h dorsal neural keel that express *isl-1* (Figs. 6G and 6H; Appel *et al.*, 1995). We counted the number of *isl-1*-expressing RB cells present in the region of the neural keel corresponding to segments 2–9 and found 52 RB cells present in 14 hemisegments of a WT embryo and 54 RB cells present in 14 hemisegments of an *aln* embryo. The development of these dorsal neurons appears completely spared in mutant embryos.

Expression of the genes marking early neural crest indicated that some neural crest was likely to be generated in mutant embryos. For example, *snail-2* expression indicated that cranial neural crest appeared less depleted than trunk

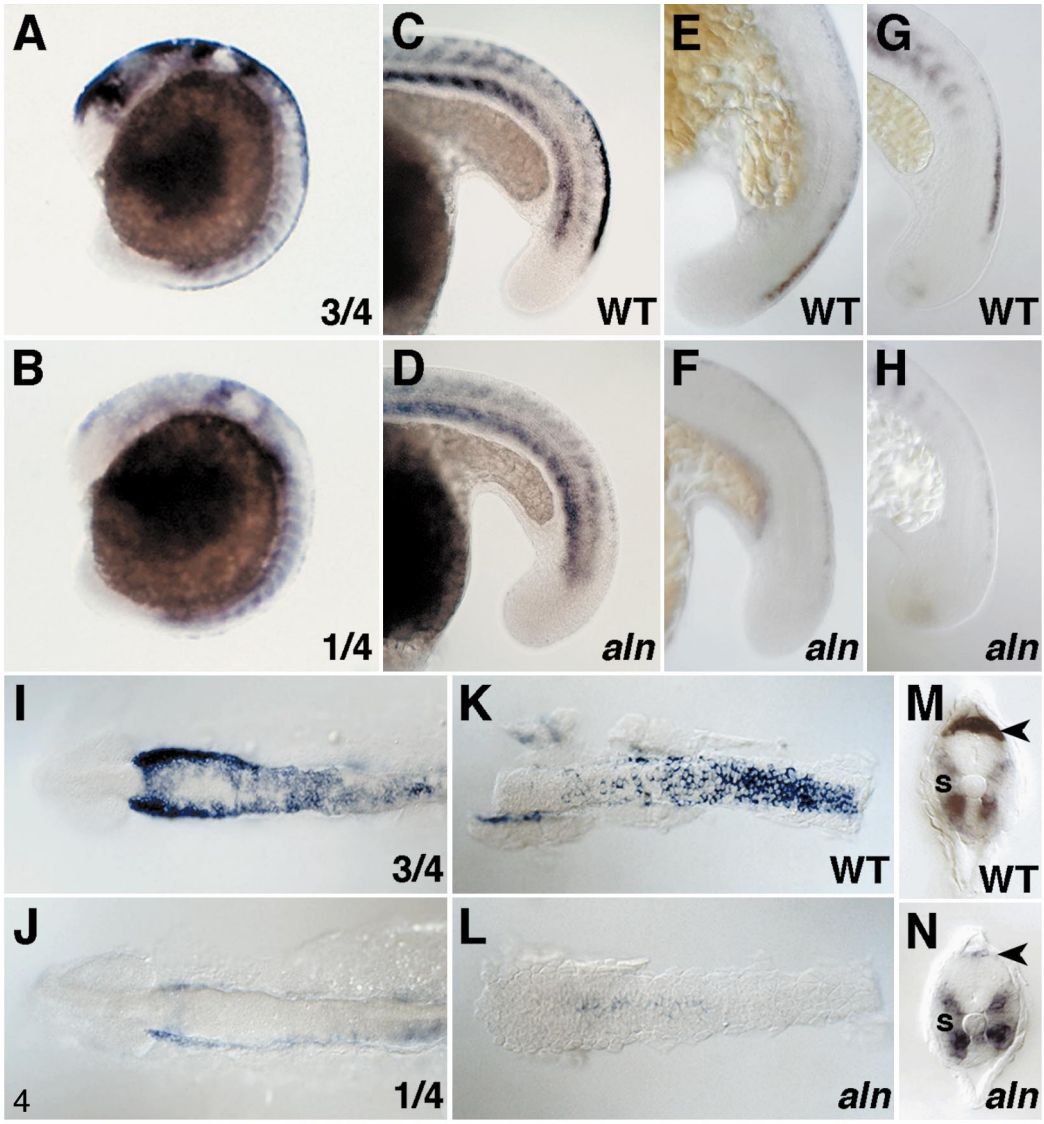

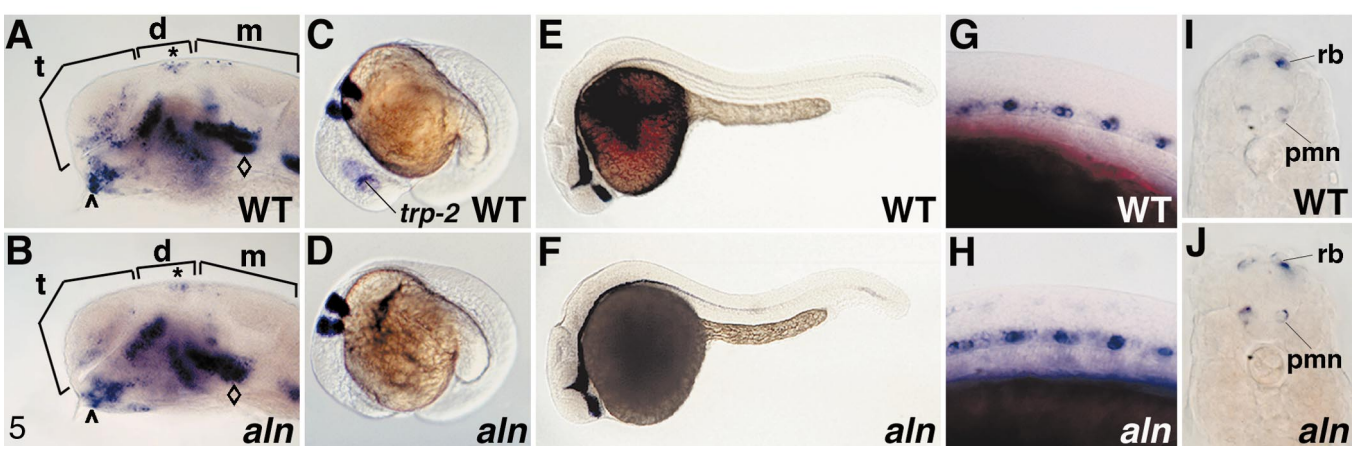

FIG. 4. Analysis of premigratory neural crest development. (A, B) One-fourth of 16-h *aln*/+ intercross progeny display a marked reduction in the expression of *snail-2* along the dorsal midline of the head and anterior trunk (B), compared to the remaining three-fourths (A). Expression of *snail-2* in the developing trunk somites is similar in the two classes. (C–H) Expression of markers for premigratory neural

neural crest (Figs. 4I–4L). Since many structures, such as branchial arches and cranial ganglia, are formed with contributions from both neural crest and nonneural crest sources, and since many of the available markers for these tissues are not specific for the neural crest-derived cells, we were unable to determine precisely the extent to which neural crest-derived tissues do form in mutant embryos. Three lines of evidence clearly indicate that some cranial neural crest can migrate out of the neural tube and differentiate in mutant embryos. First, the neural crest-derived *c-ret*-expressing precursors of the enteric nervous system are formed in *aln* mutants (Figs. 6I and 6J). Second, *goosecoid*-expressing precursors of craniofacial cartilage (Rivera-Perez *et al.*, 1995) are also present, although abnormal (Figs. 6K and 6L). Finally, direct evidence that some cranial neural crest migrates out of the neural tube in mutant embryos was obtained by labeling the dorsal hindbrain with the lipophilic vital dye DiI at the time of neural keel closure and monitoring subsequent neural crest migration under epifluorescence microscopy (Fig. 6M). Taken together, these results indicate that in *aln* mutants at least some cranial neural crest cells can migrate and differentiate into *c-ret*-expressing enteric neuron precursors, *goosecoid*-expressing cartilage precursors, but produce few, if any, chromatophores.

Molecular Analysis of the alyron Insertion

The *alyron* mutation was first detected as a recessive lethal mutation present in the SLAC113 transgenic line and has never been detected in nontransgenic members of the parental strain. The SLAC113 insertion arose after microinjection of *Eco*RI-digested pSLAC plasmid DNA (Fig. 7A) into the cytoplasm of fertilized eggs. All plasmid DNA in this line resides at a unique site since only a single pSLAC-hybridizing band was detected when DNA from heterozygous transgene carriers was digested with restriction enzymes that fail to cleave the plasmid. Following digestion with such enzymes, the smallest fragment of genomic DNA that hybridized with a plasmid probe was approximately 75 kbp (Fig. 7B). Additional Southern blot analyses of genomic DNA digested with enzymes that cleave within the plasmid sequence indicated that the insertion site contains a complex arrangement of multiple copies of the plasmid. As illustrated in Fig. 7C, digestion of heterozygous genomic DNA with *Eco*RI, an enzyme that cuts once within the plasmid, or *Bsr*DI, an enzyme that cuts at two closely spaced sites in the plasmid, yielded several size classes of fragments that hybridized with radiolabeled plasmid probe. The majority of the hybridizing DNA migrated at the size of the original plasmid (1×), indicating that most copies of the plasmid are arranged as direct repeats. Hybridizing fragments of about twice unit size (2×) were detected, consistent with fusion of plasmid units accompanied by loss of restriction sites. Other hybridizing fragments were detected at sizes consistent with the joining of unit plasmids in head-to-head or tail-to-tail orientations. In addition, fragments of unpredicted size were detected. This last class might indicate fragments spanning the junctions between the insert and host chromosome or might indicate the existence of more complex rearrangements within the plasmid sequences.

Potential junction fragments were identified in double digests of genomic DNA that generated fragments of which one end was necessarily derived from the host sequences and one end was derived from plasmid sequences. For example, digestion of heterozygous DNA with *Bsr*DI, an enzyme that cleaves within the plasmid, yielded multiple fragments that contained plasmid sequences, including a weakly hybridizing fragment of 10.5 kbp whose low abundance and unpredicted size made it a junction fragment candidate (Fig. 7C). Additional digestion of the *Bsr*DI-cut

crest in the trunk and tail of sibling WT (C, E, G) and *aln* mutant (D, F, H) 18-h embryos. Mutant embryos were identified by simultaneous staining for *trp-2* expression, which is greatly reduced in the mutant retina. Mutant embryos display severely reduced expression of *snail-2* (C, D), *AP-2* (E, F), and *fkd-6* (G, H) along the dorsal midline of the trunk and tail. (I, J) Dorsal views of the heads of 12-h *aln*/+ intercross progeny dissected from the yolk and mounted flat (anterior to the left). Expression of *snail-2* in neural crest at the edges of the anterior neural keel is reduced in one-fourth of the embryos (J) compared to the remaining three-fourths (I). (K, L) Dorsal views of neural keels dissected from 20-h *aln*/+ intercross progeny doubly stained for *trp-2* and *snail-2* (anterior is to the left). Mutant embryos display dramatically reduced *snail-2*-expression. (M, N) Transverse sections through the nascent somite of 24-h *aln*/+ intercross progeny (dorsal to the top). Mutant embryos display reduced expression of *snail-2* mRNA in the premigratory neural crest (arrowheads). Expression of *snail-2* in the somites (s) appears normal in both expression pattern and level in mutants.

FIG. 5. Analysis of rostrocaudal (A–D) and dorsoventral (E–J) patterning in the neuraxis. Prior to 24 h, *aln* mutant embryos were identified by simultaneous staining for *trp-2* expression, which is greatly reduced in the mutant retina (C, D, G, H). Expression of *zash-1A* in WT sibling (A) and *aln* mutant (B) 24-h embryos. The major compartments of the brain are indicated by brackets: telencephalon (t), diencephalon (d), and mesencephalon (m). The hypothalamus (∧), epiphysis (*), and tegmentum (◆) are also indicated. (C, D) Expression of *krox-20* in rhombomeres 3 and 5 of the hindbrain in WT sibling (C) and *aln* mutant (D) 18.5-h embryos, double stained with *trp-2* (indicated in C). (E, F) Expression of *sonic hedgehog* in the ventral brain and floor plate of WT sibling (E) and *aln* mutant (F) 24-h embryos. (G, H) Expression of *c-ret* in primary motoneurons in the ventral spinal cord of WT sibling (G) and *aln* mutant (H) 18-h embryos, double stained with *trp-2*. (I, J) Transverse sections through the midtrunk of WT sibling (I) and *aln* mutant (J) embryos stained for *isl-2* expression at 24 h. Rohon-Beard primary sensory neurons (rb) and primary motoneurons (pmn) appear normal with respect to location within the neural keel, cell body number, and expression level of *isl-2*.

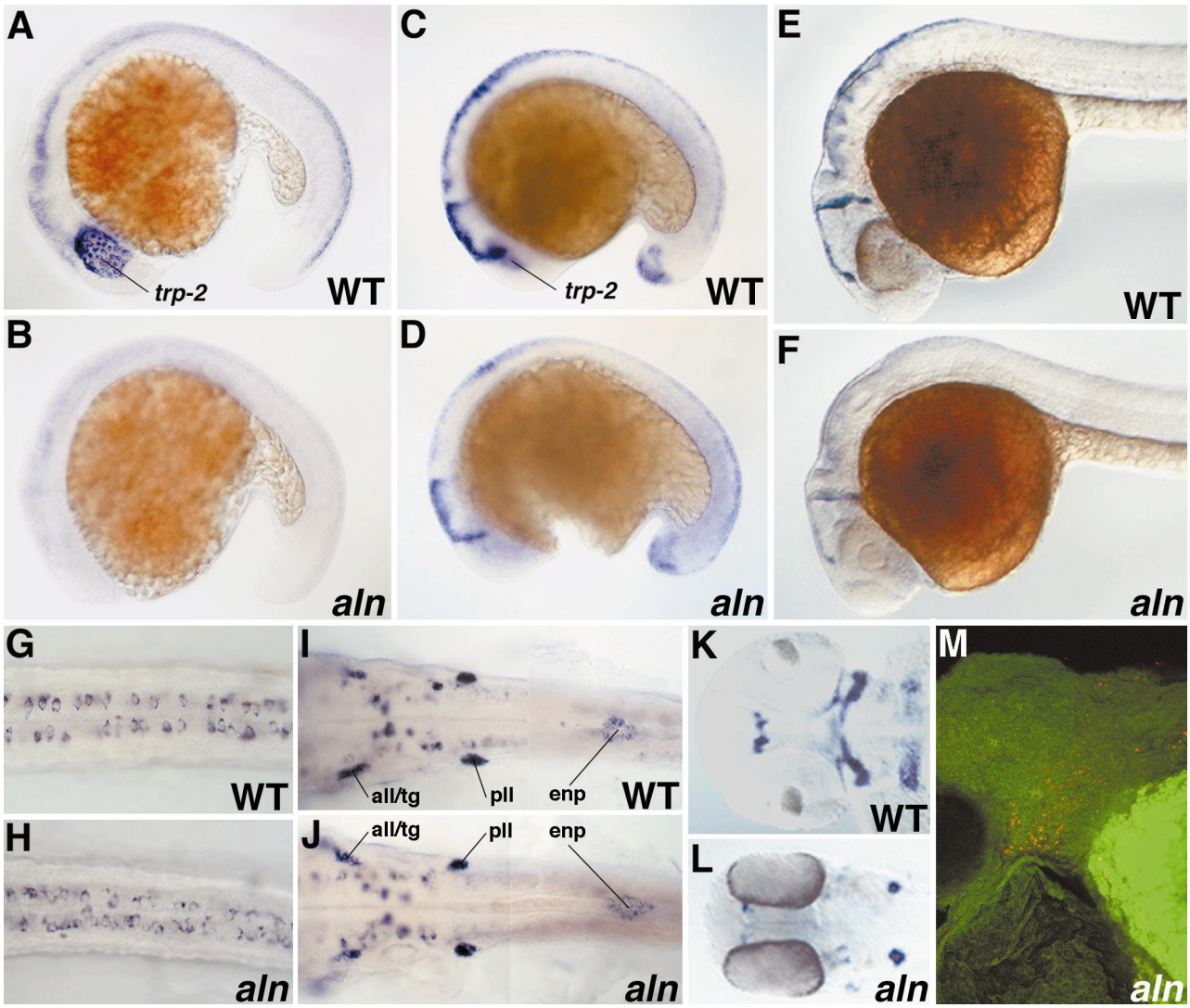

FIG. 6. Development of the dorsal neuraxis and some derivatives. Prior to 24 h, *aln* mutant embryos were identified by simultaneous staining for *trp-2* expression, which is greatly reduced in the mutant retina (A–D). (A, B) Expression of *pax-3* in the dorsal one-third of the neural keel in WT sibling (A) and *aln* mutant (B) 18.5-h embryos, double stained with *trp-2* (indicated in A). (C, D) Expression of *wnt-1* at the dorsal midline of the neural keel in WT sibling (C) and *aln* mutant (D) 18-h embryos, double stained with *trp-2* (indicated in C). (E, F) Expression of *wnt-3A* in WT sibling (E) and *aln* mutant (F) 24-h embryos. A–F indicate that several markers of dorsal neural tube identity are reduced in expression level in *aln* mutants. (G, H) *isl-1* expression in dorsal spinal cord marks Rohon-Beard primary sensory neurons in WT sibling (G) and *aln* mutant (H) 24-h embryos, shown in dorsal view with anterior to the left. (I, J) WT (I) and mutant (J) 24-h embryos exhibit similar patterns of *c-ret* expression in cranial neural crest derivatives, shown in dorsal three focal plane composite views with anterior to the left. The trigeminal (tg), anterior lateral line (all), and posterior lateral line (pll) ganglia as well as the vagal neural crest-derived precursors of the enteric nervous system (enp) are detected in *aln* mutants. (K, L) Precursors of craniofacial cartilage, marked by *goosecoid* expression at 42 h, are present in abnormally small patches in mutant embryos (L), compared to similarly staged *albino* embryos (K). (M) DiI-labeled neural crest cells (red) in the branchial arch region of a 48-h mutant embryo. DiI was applied to the neural fold at the one- to two- somite stage and the embryo was imaged under two-color confocal microscopy using a Bodipy (green) counterstain.

DNA with *Spe*I, an enzyme that cuts within the host chromosome but not the plasmid, eliminated the 10.5-kbp fragment and generated a new hybridizing fragment of 6.5 kbp (Fig. 7D).

Based on the analysis of plasmid sequences near the host *Spe*I site, a strategy utilizing linker/adapter-based PCR was devised to clone junction sequences (see Materials and Methods for details). PCR amplification yielded a 2.1-kbp product, which was cloned and sequenced. The 2.1-kbp junction fragment contained 324 bp of host sequence joined

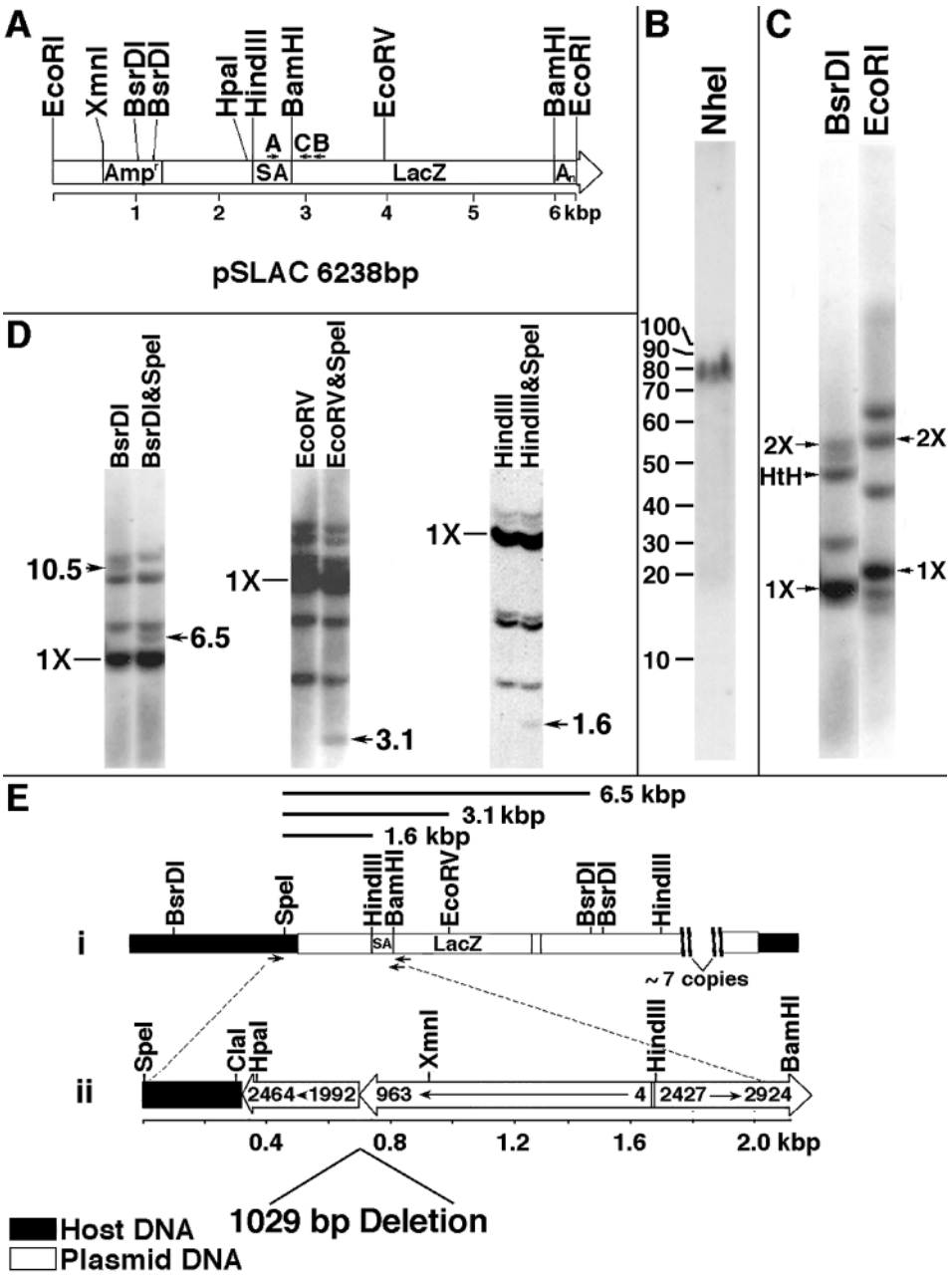

FIG. 7. Molecular characterization of the *aln* insertion. (A) Diagram of pSLAC linearized at the unique *Eco*RI site. The origins of gene sequences present in pSLAC are described under Materials and Methods. A, B, and C refer to oligomer primers used for PCR. (B) Southern blot of *aln*/+ genomic DNA digested with *Nhe*I, which does not cleave pSLAC. Digested DNA was subjected to FIGE and probed with radiolabeled pSLAC sequences. (C) Southern blot of *aln*/+ DNA digested with *Bsr*DI or *Eco*RI and probed with radiolabeled pSLAC sequences. 1X refers to unit size (6.0 kbp for *Bsr*DI, 6.2 kbp for *Eco*RI), 2X refers to twice unit size, and HtH refers to the predicted size of the *Bsr*DI fragment of two units arranged head to head. (D) Identification of host–insert junction fragments. *aln*/+ DNA was digested with the indicated enzymes, separated on 0.7 or 1% agarose gels, blotted, and probed with radiolabeled pSLAC. Candidate junction fragments are indicated by arrows with approximate sizes given in kilobasepairs. (E) Orientation of sequences at a host–insert junction. (i) Restriction map of host and plasmid-derived sequences at one junction. Junction fragments identified in D are indicated as bars above the map. Positions of primers used to amplify junction region are indicated by arrows below the map. (ii) Diagram of the 2.1-kbp junction fragment that was PCR amplified using primers denoted in i. Host-derived sequence (324 bp) is fused to portions of two plasmid units arranged tail to tail. One plasmid unit has an internal deletion of about 1 kbp, and the other plasmid unit has a terminal deletion of about 2.4 kbp. Numbers within the bars refer to basepair numbers of pSLAC indicated in A.

to 1852 bp of pSLAC-derived sequence (Fig. 7E). The host sequence appears novel and contains no open reading frame. The plasmid-derived sequence contains portions of two plasmid units arranged tail to tail, one of which displays a 1029-bp internal deletion relative to the sequence of the original plasmid. In sum, the arrangement of sequences in the *aln* insertion resembles those reported for insertions generated by DNA microinjection into mouse embryos (reviewed in Palmiter and Brinster, 1986; Gridley *et al.*, 1987; Woychik and Alagramam, 1998).

Genetic Linkage and Mapping

To test the likelihood that the insertion of plasmid sequences caused the lethal mutation, we examined the genetic linkage between the SLAC113 transgene and the *aln* mutation. In these tests we asked whether the lethal mutation and the transgene insertion cosegregated among the progeny of females that were heterozygous for both the transgene and the mutation. In one test, carriers were mated to WT partners and the somatic tissue of the F1 progeny was first analyzed for the presence of the transgene. Subsequently, the presence of the *aln* mutation in the germ line of F1 progeny was ascertained by progeny testing. Among 137 F1 progeny that harbored the transgene, all were found to have inherited the lethal mutation. Among 32 F1 progeny that did not harbor the transgene, all were found to have inherited the wild-type allele of *aln*. In a separate test, F1 progeny were first tested for inheritance of the *aln* mutation. All 40 *aln*/+ F1 progeny were subsequently shown to have inherited the transgene. Thus, in no case were the transgene and the *aln* mutation separated by meiotic recombination (0/209 recombinants). This result indicates that the transgene and the lethal mutation are very close to one another, within 1.8 cM (95% confidence limit). The simplest explanation for this observation is that the insertion of the transgene has caused the lethal mutation.

As a first step toward mapping the *aln* mutation, we identified a polymorphic genomic sequence tightly linked to the SLAC113 transgene. As expected from the sequence of the cloned junction fragment, oligomer PCR primers (J191; see Materials and Methods) complementary to the host sequences present in the junction fragment amplified a 191-bp fragment from genomic DNA prepared from homozygous *aln* mutant embryos. In contrast, two products of approximately 170 and 191 bp were amplified from *aln*/+ heterozygous DNA. To demonstrate that the genomic sequences detected by these primers were alleles and that the 191-bp product was amplified from host sequences linked to the SLAC113 transgene, we analyzed the segregation of the PCR-amplified host and transgene sequences among the haploid progeny of an *aln*/+ heterozygote. Among 63 haploid offspring analyzed, all 35 transgene carriers inherited the 191-bp allele and all 28 WT siblings inherited the 170-bp allele. Thus, the J191 primers specifically detect a genomic sequence closely linked to the *aln* locus. To map *aln*, we determined the segregation of the J191-amplified sequences in a radiation hybrid panel (Kwok *et al.*, 1998). These analyses indicated assignment of the *aln* locus to the distal arm of linkage group (LG) 15, 38 cR from markers z24 and z5223 (R. Geisler and P. Haffter, personal communication).

As the *aln* phenotype resembles that of mouse mutants lacking *Pax-3* or both *Wnt-1* and *Wnt-3a* gene functions, we determined whether *aln* was linked to zebrafish homologues of these genes. Oligomer PCR primers specific for the candidate genes were generated and the segregation of each gene sequence in the RH panel was determined. Zebrafish *pax-3* and *wnt-3a* map to LG 2, *pax-7* to LG 11, and *wnt-1* to LG 23 (segregation analysis performed in collaboration with R. Geisler and P. Haffter). *wnt-1* was mapped previously to LG 23 by Postlethwait *et al.* (1998). Since none of the candidates tested map to LG 15, *aln* cannot be a mutation in one of these genes.

DISCUSSION

Insertional Mutagenesis by DNA Microinjection into Zebrafish Eggs

The *alyron*^{z12} mutation was likely induced by insertional mutagenesis. The mutation was first detected as a recessive lethal mutation present in the SLAC113 transgenic line and has never been detected in nontransgenic members of the parental strain. The SLAC113 line was initiated by injection of linearized plasmid DNA into the cytoplasm of a one-cell zebrafish embryo and harbors multiple copies of plasmid DNA integrated at a single site in the host genome. The integrated plasmid sequences cosegregate with the *aln* mutation and linkage tests indicate that they map less than 2 cM from the mutation. Proof that the transgenic sequences have induced the mutation awaits molecular characterization of the *aln* gene in wild-type and transgenic genomes.

Published (Stuart *et al.*, 1990; Culp *et al.*, 1991; Bayer and Campos-Ortega, 1992) and unpublished (A. Alexander, J. Campos-Ortega, P. Gibbs, N. Hopkins, and M. Westerfield, personal communication) accounts of previous attempts to generate insertional mutations in the zebrafish suggest that approximately 75 transgenic lines generated by microinjection of DNA into the cytoplasm of early cleavage embryos have been tested for the presence of associated developmental mutations. The present study is the first report of a lethal mutation induced by this procedure. Thus, microinjection-mediated DNA integration might cause insertional mutations with a frequency comparable to that of proviral integrations that arise following retroviral infection of embryos (1–2%) (Allende *et al.*, 1996; Gaiano *et al.*, 1996).

The arrangement of integrated DNA sequences in the SLAC113 line is similar in many details to that of transgenes generated in the mouse by pronuclear injection of fertilized eggs (reviewed in Palmiter and Brinster, 1986; Gridley *et al.*, 1987; Woychik and Alagramam, 1998) and is

probably representative of transgenes produced by cytoplasmic injection of zebrafish early embryos (Stuart *et al.*, 1988, 1990; Culp *et al.*, 1991; Bayer and Campos-Ortega, 1992). Approximately eight copies of the plasmid have been integrated into a single host chromosome site. Many of the copies are arranged as direct repeats; however, multiple rearrangements of the plasmid sequences, including internal deletions, are also present. Given the existence of multiple plasmid copies at the site of integration and the possibility that host sequences may have been rearranged during the illegitimate recombination events that led to transgenesis, it is clear that identification of a gene disrupted by insertional mutagenesis will often be simpler following retroviral infection than following DNA microinjection.

alyron Is a New Zebrafish Mutant

Our analysis of the development of a variety of tissues and cell types in mutant embryos indicates that *alyron* is phenotypically distinct from previously described zebrafish mutants. The early reduction of premigratory neural crest along the entire axis distinguishes *aln* from most neural crest mutants (Neuhauss *et al.*, 1996; Piotrowski *et al.*, 1996; Schilling *et al.*, 1996a,b; Kelsh *et al.*, 1996; Odenthal *et al.*, 1996; Henion *et al.*, 1996; Chandrasekhar *et al.*, 1997). The effect of *aln* on the expression of dorsal but not ventral markers in the neuraxis distinguishes it from other mutations affecting dorsoventral patterning of the CNS (Jiang *et al.*, 1996; Schier *et al.*, 1996). The normal appearance and number of Rohon-Beard sensory neurons distinguish the *aln* phenotype from that of *mindbomb/whitetail* mutants (Jiang *et al.*, 1996; Schier *et al.*, 1996). The previously described mutant whose phenotype most resembles that of *aln* is *colourless* (Kelsh *et al.*, 1996). *colourless* displays pigmentation and ear morphology defects similar to those displayed by *aln*, but genetic complementation tests reveal that these mutations are nonallelic (C. J. Cretekos and R. Kelsh, unpublished observations).

alyron Has an Early Defect in Neural Crest Development

Many tissues are affected in mutant embryos, including the chromatophores, the heart, the ear, and the CNS. It is possible that the integration of plasmid sequences in the SLAC113 line disrupted several gene functions, thereby accounting for the pleiotropic defects exhibited by mutants. Our results indicate that there is no compelling reason to invoke this possibility. Many of the developmental abnormalities observed in *alyron* mutants can be traced to a single primary defect: a reduction in the premigratory neural crest. Analysis of *snail-2*, *AP-2*, and *fkd-6* expression indicated that premigratory neural crest was reduced along the entire rostrocaudal axis of mutant embryos, being nearly absent from the trunk and the tail. This finding readily accounts for the absence of melanophores, xanthophores, and HU antigen-positive dorsal root ganglia (C. J. Cretekos and R. Kelsh, unpublished observations) in *aln* mutants. Reduction in neural crest contributions could also be responsible for the aberrant morphogenesis of the ear in mutants, given that mutations in 14 other loci affecting neural crest development in zebrafish display a similar ear defect (Malicki *et al.*, 1996; Whitfield *et al.*, 1996). In addition, our findings indicate that the failure of blood to circulate probably results from the inability of mutant hearts to effect the directional movement of fluid. This defect might be secondary to a deficit in a neural crest contribution to the heart. We have found that neural crest descendants normally migrate into the heart in zebrafish (Cretekos, 1998), as they do in other vertebrates, and analysis of the *Splotch* (*Pax-3*) mutant indicates that the neural crest contribution is required for effective heart function in the mouse (Conway *et al.*, 1997). Molecular markers specific for the cardiac neural crest in zebrafish are required to determine directly whether *aln* mutants are deficient in this tissue.

Although several neural crest lineages are affected in *aln* mutants, some tissues derived from the neural crest are unaffected or only mildly affected in mutants. Because mutant embryos exhibit developmental delay beginning at about 22 h of development and die at about 3 days, it is impossible to assess the ultimate differentiation of many neural crest-derived tissues in mutants. The neural crest-derived precursors of the enteric nervous system, which are uniquely identifiable by their positions and their expression of the *c-ret* gene (Bisgrove *et al.*, 1997; Marcos-Gutierrez *et al.*, 1997), appear to be formed normally in mutant embryos. Similarly, cranial ganglia that are formed in part with neural crest contributions appear normal or only slightly reduced in size in mutants compared with WT embryos (Figs. 6I and 6L). Finally, *goosecoid*-expressing precursors of head cartilage are generated, although abnormal. The finding that no mutant specifically lacking all neural crest tissue has been described in any vertebrate may mean that multiple genetic pathways regulate induction of the neural crest or that factors essential for all neural crest are also required for the ontogeny of other early-arising tissues.

Role of alyron in Neural Crest and Dorsal Neural Keel Development

alyron mutants have a severe deficit but not a complete absence of premigratory neural crest. Despite Aristotle's advice that "he who considers things in their first growth and origin . . . will obtain the clearest view of them" (Aristotle, Politics, Book 1, Chapter 2), the mutant phenotype does not reveal precisely what role the gene has in neural crest development. Lack of *aln* function could compromise the full induction, establishment of identity, or proliferative expansion of the early neural crest.

Induction of the neural crest appears to require signaling via BMP, FGF, and Wnt growth factors (reviewed in Baker and Bronner-Fraser, 1997; LaBonne and Bronner-Fraser, 1998). As

mesodermal and neural patterning appears normal in *aln* mutants, it is unlikely that the mutation widely affects BMP or FGF signaling in the embryo. Given our results indicating that *aln* is required cell autonomously for chromatophore development, it is likely that *aln* functions within the earliest cells of the neural crest lineage. Thus, if the mutation blocks the induction process, *aln* might encode a neural-specific receptor for one of these growth factors.

If *aln* functions downstream of the inductive signals, the coordinate effects of the mutation on *Pax* and *Wnt* gene expression make it difficult to distinguish a role in specification from a role in proliferative expansion. The dorsal neural tube phenotype of *aln* strongly resembles that seen in both the mouse *Pax-3* and the mouse *Wnt-1/Wnt-3a* double mutant. Lack of melanocytes and cardiac neural crest is characteristic of the *Pax-3* mutant. Similarly, the *aln* phenotype resembles the *Wnt-1/Wnt-3a* mutant in several respects. Both mutants exhibit a severe reduction of pigment cells, but only a partial reduction of other neural crest-derived tissues. Overall, dorsoventral patterning appears spared in both mutants, but dorsal neural tube identity as measured by the level of *Pax-3* gene expression appears compromised in both mutants. Finally, in addition to the defects that can be traced readily to the neural crest, other aspects of development appear similarly affected in the zebrafish and mouse mutants. For example, both mutants display developmental retardation, and both mutants appear to have abnormal cell death in the brain.

The finding that expression of both *Wnt* and *Pax* genes in the dorsal neural tube is reduced in the *aln* mutant and in the mouse *Wnt-1/Wnt-3a* double mutant (Ikeya *et al.*, 1997) suggests that *Wnt* signaling and *Pax* gene function regulate each other. Given that aln^{z12} is unlinked to zebrafish *Pax* or *Wnt* genes known to be expressed in the dorsal neural keel, the *aln* mutation identifies a novel gene function. *aln* may encode a factor necessary for transmission of *Pax* gene function or *Wnt* signaling in the dorsal neural keel. Alternatively, *aln* may identify a new pathway that regulates *Pax* and *Wnt* gene expression. Molecular analysis of the gene will facilitate distinguishing these possibilities.

ACKNOWLEDGMENTS

We thank Mario Capecchi, Chi-Bin Chien, Robert Kelsh, Charles Kimmel, David Raible, Mahendra Rao, Gary Schoenwolf, Carl Thummel, and our laboratory colleagues for their critical advice and their help with the analysis of the *alyron* mutant phenotype. We have benefited from excellent technical assistance provided by Virginia Walter and Sharon Johnson. We thank numerous colleagues in the field who generously provided, often prior to publication, clones and sequences that were used for *in situ* hybridization analyses and linkage analyses. We especially thank R. Kelsh for providing *trp-2* and for HU immunohistochemistry, H. Seo and A. Fjose for providing *pax-3* and *pax-7,* R. Dorsky and R. Moon for providing *wnt-1* and *wnt-3a,* and R. Geisler and P. Haffter for assistance with RH mapping. This work was supported by grants from NSF (DCB-9105585 and MCB-9420984).

REFERENCES

Akimenko, M. A., Ekker, M., Wegner, J., Lin, W., and Westerfield, M. (1994). Combinatorial expression of three zebrafish genes related to distal-less: Part of a homeobox gene code for the head. *J. Neurosci.* **14,** 3475–3486.

Allende, M. L., Amsterdam, A., Becker, T., Kawakami, K., Gaiano, N., and Hopkins, N. (1996). Insertional mutagenesis in zebrafish identifies two novel genes, pescadillo and dead eye, essential for embryonic development. *Genes Dev.* **10,** 3141–3155.

Allende, M. L., and Weinberg, E. S. (1994). The expression pattern of two zebrafish achaete–scute homolog (ash) genes is altered in the embryonic brain of the cyclops mutant. *Dev. Biol.* **166,** 509–530.

Anderson, D. J. (1997). Cellular and molecular biology of neural crest cell lineage determination. *Trends Genet.* **13,** 276–280.

Appel, B., Korzh, V., Glasgow, E., Thor, S., Edlund, T., Dawid, I. B., and Eisen, J. S. (1995). Motoneuron fate specification revealed by patterned LIM homeobox gene expression in embryonic zebrafish. *Development* **121,** 4117–4125.

Auerbach, R. (1954). Analysis of the developmental effects of the lethal mutation in the house mouse. *J. Exp. Zool.* **127,** 305–329.

Augustine, K., Liu, E. T., and Sadler, T. W. (1993). Antisense attenuation of Wnt-1 and Wnt-3a expression in whole embryo culture reveals roles for these genes in craniofacial, spinal cord, and cardiac morphogenesis. *Dev. Genet.* **14,** 500–520.

Ausubel, F. M., Brent, R., Kingston, R. E., Moore, D. D., Seidman, J. G., Smith, J. A., and Struhl, K. (1989). "Current Protocols in Molecular Biology." Wiley, New York.

Baker, C. V., and Bronner-Fraser, M. (1997). The origins of the neural crest. Part I: Embryonic induction. *Mech. Dev.* **69,** 3–11.

Bayer, T. A., and Campos-Ortega, J. A. (1992). A transgene containing lacZ is expressed in primary sensory neurons in zebrafish. *Development* **115,** 421–426.

Besmer, P., Manova, K., Duttlinger, R., Huang, E. J., Packer, A., Gyssler, C., and Bachvarova, R. F. (1993). The kit-ligand (steel factor) and its receptor c-kit/W: Pleiotropic roles in gametogenesis and melanogenesis. *Dev. Suppl.,* 125–137.

Bisgrove, B. W., Raible, D. W., Walter, V., Eisen, J. S., and Grunwald, D. J. (1997). Expression of c-ret in the zebrafish embryo: Potential roles in motoneuronal development. *J. Neurobiol.* **33,** 749–768.

Chandrasekhar, A., Moens, C. B., Warren, J. T., Jr., Kimmel, C. B., and Kuwada, J. Y. (1997). Development of branchiomotor neurons in zebrafish. *Development* **124,** 2633–2644.

Chang, C., and Hemmati-Brivanlou, A. (1998). Neural crest induction by Xwnt7B in *Xenopus. Dev. Biol.* **194,** 129–134.

Conway, S. J., Henderson, D. J., and Copp, A. J. (1997). Pax3 is required for cardiac neural crest migration in the mouse. *Development* **124,** 505–514.

Cooper, M. S., and D'Amico, L. A. (1996). A cluster of noninvoluting endocytic cells at the margin of the zebrafish blastoderm marks the site of embryonic shield formation. *Dev. Biol.* **180,** 184–198.

Creazzo, T. L., Godt, R. E., Leatherbury, L., Conway, S. J., and Kirby, M. L. (1998). Role of cardiac neural crest cells in cardiovascular development. *Annu. Rev. Physiol.* **60,** 267–286.

Cretekos, C. J. (1998). Contribution of early cell movements and formation of the neural crest to zebrafish embryogenesis. Ph.D. thesis, Univ. Utah.

Culp, P., Nusslein-Volhard, C., and Hopkins, N. (1991). High-frequency germ-line transmission of plasmid DNA sequences injected into fertilized zebrafish eggs. *Proc. Natl. Acad. Sci. USA* **88,** 7953–7957.

Dorsky, R. I., Moon, R. T., and Raible, D. W. (1998). Control of neural crest cell fate by the Wnt signalling pathway. *Nature* **396,** 370–373.

Epperlein, H. H., Ziegler, I., and Perris, R. (1988). Identification of pigment cells during early amphibian development (*Triturus alpestris, Ambystoma mexicanum*). *Cell Tissue Res.* **253,** 493–505.

Epstein, D. J., Vekemans, M., and Gros, P. (1991). Splotch (Sp2H), a mutation affecting development of the mouse neural tube, shows a deletion within the paired homeodomain of Pax-3. *Cell* **67,** 767–774.

Fleischman, R. A. (1993). From white spots to stem cells: The role of the Kit receptor in mammalian development. *Trends Genet.* **9,** 285–290.

Franz, T., and Kothary, R. (1993). Characterization of the neural crest defect in Splotch (Sp1H) mutant mice using a lacZ transgene. *Brain Res. Dev. Brain Res.* **72,** 99–105.

Furthauer, M., Thisse, C., and Thisse, B. (1997). A role for FGF-8 in the dorsoventral patterning of the zebrafish gastrula. *Development* **124,** 4253–4264.

Gaiano, N., Amsterdam, A., Kawakami, K., Allende, M., Becker, T., and Hopkins, N. (1996). Insertional mutagenesis and rapid cloning of essential genes in zebrafish. *Nature* **383,** 829–832.

Garton, H. J., and Schoenwolf, G. C. (1996). Improving the efficacy of fluorescent labeling for histological tracking of cells in early mammalian and avian embryos. *Anat. Rec.* **244,** 112–117.

Gridley, T., Soriano, P., and Jaenisch, R. (1987). Insertional mutagenesis in mice. *Trends Genet.* **3,** 162–166.

Grunwald, D. J., Kimmel, C. B., Westerfield, M., Walker, C., and Streisinger, G. (1988). A neural degeneration mutation that spares primary neurons in the zebrafish. *Dev. Biol.* **126,** 115–128.

Henion, P. D., Raible, D. W., Beattie, C. E., Stoesser, K. L., Weston, J. A., and Eisen, J. S. (1996). Screen for mutations affecting development of zebrafish neural crest. *Dev. Genet.* **18,** 11–17.

Ho, R. K., and Kimmel, C. B. (1993). Commitment of cell fate in the early zebrafish embryo. *Science* **261,** 109–111.

Hong, R. (1998). The DiGeorge anomaly (CATCH 22, DiGeorge/velocardiofacial syndrome). *Semin. Hematol.* **35,** 282–290.

Hug, B., Walter, V., and Grunwald, D. J. (1997). tbx6, a Brachyury-related gene expressed by ventral mesendodermal precursors in the zebrafish embryo. *Dev. Biol.* **183,** 61–73.

Ikeya, M., Lee, S. M., Johnson, J. E., McMahon, A. P., and Takada, S. (1997). Wnt signalling required for expansion of neural crest and CNS progenitors. *Nature* **389,** 966–970.

Inoue, A., Takahashi, M., Hatta, K., Hotta, Y., and Okamoto, H. (1994). Developmental regulation of islet-1 mRNA expression during neuronal differentiation in embryonic zebrafish. *Dev. Dyn.* **199,** 1–11.

Jiang, Y. J., Brand, M., Heisenberg, C. P., Beuchle, D., Furutani-Seiki, M., Kelsh, R. N., Warga, R. M., Granato, M., Haffter, P., Hammerschmidt, M., Kane, D. A., Mullins, M. C., Odenthal, J., van Eeden, F. J., and Nusslein-Volhard, C. (1996). Mutations affecting neurogenesis and brain morphology in the zebrafish, *Danio rerio*. *Development* **123,** 205–216.

Kelsh, R. N., Brand, M., Jiang, Y. J., Heisenberg, C. P., Lin, S., Haffter, P., Odenthal, J., Mullins, M. C., van Eeden, F. J., Furutani-Seiki, M., Granato, M., Hammerschmidt, M., Kane, D. A., Warga, R. M., Beuchle, D., Vogelsang, L., and Nusslein-Volhard, C. (1996). Zebrafish pigmentation mutations and the processes of neural crest. *Development* **123,** 369–389.

Kimmel, C. B., and Warga, R. M. (1987). Indeterminate cell lineage of the zebrafish embryo. *Dev. Biol.* **124,** 269–280.

Krauss, S., Concordet, J. P., and Ingham, P. W. (1993). A functionally conserved homolog of the *Drosophila* segment polarity gene hh is expressed in tissues with polarizing activity in zebrafish embryos. *Cell* **75,** 1431–1444.

Kwok, C., Korn, R. M., Davis, M. E., Burt, D. W., Critcher, R., McCarthy, L., Paw, B. H., Zon, L. I., Goodfellow, P. N., and Schmitt, K. (1998). Characterization of whole genome radiation hybrid mapping resources for non-mammalian vertebrates. *Nucleic Acids Res.* **26,** 3562–3566.

LaBonne, C., and Bronner-Fraser, M. (1998). Neural crest induction in *Xenopus:* Evidence for a two-signal model. *Development* **125,** 2403–2414.

Le Douarin, N. (1982). "The Neural Crest." Cambridge Univ. Press, New York.

Lee, R. K., Stainier, D. Y., Weinstein, B. M., and Fishman, M. C. (1994). Cardiovascular development in the zebrafish. II. Endocardial progenitors are sequestered within the heart field. *Development* **120,** 3361–3366.

Lewis, J. (1996). Neurogenic genes and vertebrate neurogenesis. *Curr. Opin. Neurobiol.* **6,** 3–10.

Liao, W., Bisgrove, B. W., Sawyer, H., Hug, B., Bell, B., Peters, K., Grunwald, D. J., and Stainier, D. Y. (1997). The zebrafish gene cloche acts upstream of a flk-1 homologue to regulate endothelial cell differentiation. *Development* **124,** 381–389.

Liem, K. F., Jr., Tremml, G., and Jessell, T. M. (1997). A role for the roof plate and its resident TGFbeta-related proteins in neuronal patterning in the dorsal spinal cord. *Cell* **91,** 127–138.

Liem, K. F., Jr., Tremml, G., Roelink, H., and Jessell, T. M. (1995). Dorsal differentiation of neural plate cells induced by BMP-mediated signals from epidermal ectoderm. *Cell* **82,** 969–979.

Malicki, J., Schier, A. F., Solnica-Krezel, L., Stemple, D. L., Neuhauss, S. C., Stainier, D. Y., Abdelilah, S., Rangini, Z., Zwartkruis, F., and Driever, W. (1996). Mutations affecting development of the zebrafish ear. *Development* **123,** 275–283.

Mansouri, A., Stoykova, A., Torres, M., and Gruss, P. (1996). Dysgenesis of cephalic neural crest derivatives in Pax7−/− mutant mice. *Development* **122,** 831–838.

Marcos-Gutierrez, C. V., Wilson, S. W., Holder, N., and Pachnis, V. (1997). The zebrafish homologue of the ret receptor and its pattern of expression during embryogenesis. *Oncogene* **14,** 879–889.

Marusich, M. F., Furneaux, H. M., Henion, P. D., and Weston, J. A. (1994). Hu neuronal proteins are expressed in proliferating neurogenic cells. *J. Neurobiol.* **25,** 143–155.

Mayor, R., Guerrero, N., and Martinez, C. (1997). Role of FGF and noggin in neural crest induction. *Dev. Biol.* **189,** 1–12.

Mayor, R., Morgan, R., and Sargent, M. G. (1995). Induction of the prospective neural crest of *Xenopus*. *Development* **121,** 767–777.

Mehler, M. F., Mabie, P. C., Zhang, D., and Kessler, J. A. (1997). Bone morphogenetic proteins in the nervous system. *Trends Neurosci.* **20,** 309–317.

Molven, A., Njolstad, P. R., and Fjose, A. (1991). Genomic structure and restricted neural expression of the zebrafish wnt-1 (int-1) gene. *EMBO J.* **10,** 799–807.

Monaco, A. P. (1995). "Pulsed Field Gel Electrophoresis: A Practical Approach." IRL Press, New York.

Morgan, R., and Sargent, M. G. (1997). The role in neural patterning of translation initiation factor eIF4AII: Induction of neural fold genes. *Development* **124,** 2751–2760.

Neuhauss, S. C., Solnica-Krezel, L., Schier, A. F., Zwartkruis, F., Stemple, D. L., Malicki, J., Abdelilah, S., Stainier, D. Y., and Driever, W. (1996). Mutations affecting craniofacial development in zebrafish. *Development* **123,** 357–367.

Nguyen, V. H., Schmid, B., Trout, J., Connors, S. A., Ekker, M., and Mullins, M. C. (1998). Ventral and lateral regions of the zebrafish gastrula, including the neural crest progenitors, are established by a bmp2b/swirl pathway of genes. *Dev. Biol.* **199,** 93–110.

Nieto, M. A., Sargent, M. G., Wilkinson, D. G., and Cooke, J. (1994). Control of cell behavior during vertebrate development by Slug, a zinc finger gene. *Science* **264,** 835–839.

Odenthal, J., and Nusslein-Volhard, C. (1998). Fork head domain genes in zebrafish. *Dev. Genes Evol.* **208,** 245–258.

Odenthal, J., Rossnagel, K., Haffter, P., Kelsh, R. N., Vogelsang, E., Brand, M., van Eeden, F. J., Furutani-Seiki, M., Granato, M., Hammerschmidt, M., Heisenberg, C. P., Jiang, Y. J., Kane, D. A., Mullins, M. C., and Nusslein-Volhard, C. (1996). Mutations affecting xanthophore pigmentation in the zebrafish, *Danio*. *Development* **123,** 391–398.

Oxtoby, E., and Jowett, T. (1993). Cloning of the zebrafish krox-20 gene (krx-20) and its expression during hindbrain development. *Nucleic Acids Res.* **21,** 1087–1095.

Palmiter, R. D., and Brinster, R. L. (1986). Germ-line transformation of mice. *Annu. Rev. Genet.* **20,** 465–499.

Piotrowski, T., Schilling, T. F., Brand, M., Jiang, Y. J., Heisenberg, C. P., Beuchle, D., Grandel, H., van Eeden, F. J., Furutani-Seiki, M., Granato, M., Haffter, P., Hammerschmidt, M., Kane, D. A., Kelsh, R. N., Mullins, M. C., Odenthal, J., Warga, R. M., and Nusslein-Volhard, C. (1996). Jaw and branchial arch mutants in zebrafish II: Anterior arches and cartilage differentiation. *Development* **123,** 345–356.

Postlethwait, J. H., Yan, Y. L., Gates, M. A., Horne, S., Amores, A., Brownlie, A., Donovan, A., Egan, E. S., Force, A., Gong, Z., Goutel, C., Fritz, A., Kelsh, R., Knapik, E., Liao, E., Paw, B., Ransom, D., Singer, A., Thomson, M., Abduljabbar, T. S., Yelick, P., Beier, D., Joly, J. S., Larhammar, D., Rosa, F., *et al.* (1998). Vertebrate genome evolution and the zebrafish gene map. *Nat. Genet.* **18,** 345–349.

Read, A. P., and Newton, V. E. (1997). Waardenburg syndrome. *J. Med. Genet.* **34,** 656–665.

Reed, R., and Maniatis, T. (1986). A role for exon sequences and splice-site proximity in splice-site selection. *Cell* **46,** 681–690.

Riley, B. B., and Grunwald, D. J. (1995). Efficient induction of point mutations allowing recovery of specific locus mutations in zebrafish. *Proc. Natl. Acad. Sci. USA* **92,** 5997–6001.

Rivera-Perez, J. A., Mallo, M., Gendron-Maguire, M., Gridley, T., and Behringer, R. R. (1995). Goosecoid is not an essential component of the mouse gastrula organizer but is required for craniofacial and rib development. *Development* **121,** 3005–3012.

Saint-Jeannet, J. P., He, X., Varmus, H. E., and Dawid, I. B. (1997). Regulation of dorsal fate in the neuraxis by Wnt-1 and Wnt-3a. *Proc. Natl. Acad. Sci. USA* **94,** 13713–13718.

Sambrook, J., Fritsch, E. F., and Maniatis, T. (1989). "Molecular Cloning: A Laboratory Manual." Cold Spring Harbor Laboratory Press, Cold Spring Harbor, NY.

Schier, A. F., Neuhauss, S. C., Harvey, M., Malicki, J., Solnica-Krezel, L., Stainier, D. Y., Zwartkruis, F., Abdelilah, S., Stemple, D. L., Rangini, Z., Yang, H., and Driever, W. (1996). Mutations affecting the development of the embryonic zebrafish brain. *Development* **123,** 165–178.

Schilling, T. F. (1997). Genetic analysis of craniofacial development in the vertebrate embryo. *Bioessays* **19,** 459–468.

Schilling, T. F., Walker, C., and Kimmel, C. B. (1996a). The chinless mutation and neural crest cell interactions in zebrafish. *Development* **122,** 1417–1426.

Schilling, T. F., Piotrowski, T., Grandel, H., Brand, M., Heisenberg, C. P., Jiang, Y. J., Beuchle, D., Hammerschmidt, M., Kane, D. A., Mullins, M. C., van Eeden, F. J., Kelsh, R. N., Furutani-Seiki, M., Granato, M., Haffter, P., Odenthal, J., Warga, R. M., Trowe, T., and Nusslein-Volhard, C. (1996b). Jaw and branchial arch mutants in zebrafish. I: Branchial arches. *Development* **123,** 329–344.

Sechrist, J., Nieto, M. A., Zamanian, R. T., and Bronner-Fraser, M. (1995). Regulative response of the cranial neural tube after neural fold ablation: Spatiotemporal nature of neural crest regeneration and up-regulation of Slug. *Development* **121,** 4103–4115.

Seo, H. C., Saetre, B. O., Havik, B., Ellingsen, S., and Fjose, A. (1998). The zebrafish Pax3 and Pax7 homologues are highly conserved, encode multiple isoforms and show dynamic segment-like expression in the developing brain. *Mech. Dev.* **70,** 49–63.

Serbedzija, G. N., and McMahon, A. P. (1997). Analysis of neural crest cell migration in Splotch mice using a neural crest-specific LacZ reporter. *Dev. Biol.* **185,** 139–147.

Stachel, S. E., Grunwald, D. J., and Myers, P. Z. (1993). Lithium perturbation and goosecoid expression identify a dorsal specification pathway in the pregastrula zebrafish. *Development* **117,** 1261–1274.

Stuart, G. W., McMurray, J. V., and Westerfield, M. (1988). Replication, integration and stable germ-line transmission of foreign sequences injected into early zebrafish embryos. *Development* **103,** 403–412.

Stuart, G. W., Vielkind, J. R., McMurray, J. V., and Westerfield, M. (1990). Stable lines of transgenic zebrafish exhibit reproducible patterns of transgene expression. *Development* **109,** 577–584.

Thisse, C., Thisse, B., and Postlethwait, J. H. (1995). Expression of snail2, a second member of the zebrafish snail family, in cephalic mesendoderm and presumptive neural crest of wild-type and spadetail mutant embryos. *Dev. Biol.* **172,** 86–99.

Tremblay, P., Kessel, M., and Gruss, P. (1995). A transgenic neuroanatomical marker identifies cranial neural crest deficiencies associated with the Pax3 mutant Splotch. *Dev. Biol.* **171,** 317–329.

Trevarrow, B., Marks, D. L., and Kimmel, C. B. (1990). Organization of hindbrain segments in the zebrafish embryo. *Neuron* **4,** 669–679.

Vooijs, M., Yu, L. C., Tkachuk, D., Pinkel, D., Johnson, D., and Gray, J. W. (1993). Libraries for each human chromosome, constructed from sorter-enriched chromosomes by using linker-adaptor PCR. *Am. J. Hum. Genet.* **52,** 586–597.

Westerfield, M. (1994). "The Zebrafish Book: A Guide for the Laboratory Use of Zebrafish (*Brachydanio rerio*)." Univ. Oregon Press, Eugene.

Whitfield, T. T., Granato, M., van Eeden, F. J., Schach, U., Brand, M., Furutani-Seiki, M., Haffter, P., Hammerschmidt, M., Heisenberg, C. P., Jiang, Y. J., Kane, D. A., Kelsh, R. N., Mullins, M. C., Odenthal, J., and Nusslein-Volhard, C. (1996). Mutations affecting development of the zebrafish inner ear and lateral line. *Development* **123,** 241–254.

Woo, K., and Fraser, S. E. (1995). Order and coherence in the fate map of the zebrafish nervous system. *Development* **121,** 2595–2609.

Woychik, R. P., and Alagramam, K. (1998). Insertional mutagenesis in transgenic mice generated by the pronuclear microinjection procedure. *Int. J. Dev. Biol.* **42,** 1009–1017.

Received for publication January 27, 1999
Revised March 25, 1999
Accepted March 29, 1999